High rate laser micro processing using high brilliant cw laser radiation

Horst EXNER, Lars HARTWIG, Robby EBERT, Sascha KLOETZER, Andre STREEK,
Joerg SCHILLE, Udo LOESCHNER

University of Applied Sciences Mittweida, Laser Application Centre,
Technikumplatz 17, 09648 Mittweida, Germany
E-mail: exner@hs-mittweida.de

Laser machining using a combination of a high power single mode cw fibre laser and fast and ultra fast scan systems, such as galvo and polygon scanner, as innovative key technologies in high rate ablation was investigated. Therefore maximum cw laser power up to 3 kW at scan speeds up to 18,000 m/min was applied. Focusing the laser beam into a laser spot of 21 µm diameter resulted in a laser dwell time less than 100 nanoseconds. Consequently laser intensities in the range of 10^8 W/cm² comparable to q-switched ns laser technology were irradiated onto stainless steel, copper, and tungsten. The paper discusses the influence of significant laser processing parameters, such as laser power, scan speed and scan number, onto ablation rate and machining qualities. Furthermore first ablation structures and micro-slits will be presented.

Keywords: high rate, laser ablation, brilliant laser, micro processing, ultra fast, polygon scanner

1. Introduction

Application of high power continuous wave laser radiation in the fields of laser micro processing requires high brilliant laser beam qualities and considerably reduced laser dwell times. Otherwise, at longer dwell times, irradiation of high laser energies causes material melting and deep penetration effects accompanied by material bulges and burr formations [1-3]. Short laser material interaction times can be realised by small focus spot sizes and ultra fast beam deflection. Furthermore the laser intensity must be high enough for material ablation. The use of commercial available high brilliant fibre laser systems with laser output power up to some kW facilitate small focus spot sizes and laser intensities of 10^8 W/cm² onto the work piece. Fast and ultra fast laser beam deflection provides innovative scan systems, such as galvanometer scanner and polygon mirror scanner technology.

In this study application of high rate cw laser ablation with laser dwell time less than 100 ns and laser intensities in the range of q-switched lasers was investigated. The influence of the processing parameters onto the ablation process will be discussed by means of stainless steel, copper and tungsten metal sheets and processing examples will be presented.

2. Experimental details

In the experiments a high brilliant single mode fibre laser YLR-3000 SM (IPG) was applied. Maximum cw laser output power of randomised polarised laser radiation was 3 kW with a times-diffraction-limit-factor of $M^2 < 1.2$. Laser beam switching frequency was 2 kHz and the minimal laser on time 250 µs. Significant laser parameter summarises Table 1.

Fast and ultra fast laser beam deflection was reached by implementation of both, a high aperture galvanometer scanner (Superscan SC-30-Y-Dig2, Raylase) and a polygon mirror scanner.

Table 1: Laser parameter.

wavelength	min. pulse duration	pulse repetition frequency
λ [nm]	t [µs]	f [kHz]
1070	250	cw - max. 2 kHz

The special designed polygon scanner consists of a polygon mirror (BFI Optilas, Lincoln Laser) for ultra fast beam deflection in X-direction and a galvanometer mirror to move up the laser beam in Y-direction. The experimental setup completed a 230 mm telecentrical f-theta objective to focus the laser beam. Technical details of the scanner systems summarises Table 2.

Table 2: Technical data of the scan systems.

	Polygon mirror scanner	Galvanometer scanner
focal distance [mm]	230	230
laser spot size d_{86} [µm]	21	21
max. scanning velocity [m/min]	18,000	1,200
max. laser power onto work piece [kW]	1.99	2.64
max. intensity onto work piece [W/cm²]	$5.7*10^8$	$7.6*10^8$
min. dwell time [µs]	0.07	1.05

Laser ablation experiments were conducted using different materials, such as 1 mm thick stainless steel 1.4301, 1 mm thick copper, and 0.5 mm thick tungsten metal sheets. Always the laser beam was focused onto the sample surface. Ablation cavities were produced by multiple line-scans of 50 mm length. Periodically after each ablated sin-

gle structure, the laser process was interrupted by a time delay of 500 ms to prevent thermal effects, caused by the overheating of the focusing optic.

Ablation structures were evaluated by means of cross section photographs, taken by a digital microscopy (VHX-100, Keyence). Therefore the ablation depths and the clear ablated areas were determined to calculate the ablation rates. However, re-deposition and re-solidification of molten material reduce the ablation depth and the ablated cross sectional area and result in lowered ablation rates.

3. Results and discussion

3.1 Characteristics and effects using ultra fast scan speed

Application of ultra fast scan systems with scan speeds faster than 1,000 m/min together with small focus spot sizes causes short dwell times of the laser beam onto the material surface. The laser dwell time can be estimated by dividing the laser spot size by the laser scanning speed. Table 3 illustrates laser dwell times achieved at different scan speeds; laser spot size was assumed of 21 µm.

Table 3: Laser dwell time at different scan speed.

scan speed [m/min]	laser dwell time [ns]
1,200	1050
2,250	560
4,500	280
9,000	140
13,500	93
18,000	70

Primarily during the experiments, ablation behaviour comparably to short pulsed laser material processing was observed. Despite the high irradiated laser intensities, the laser dwell times seems to be too short for sufficient laser energy deposition to evaporate the impinged material due to high processing speeds. Hence the influence of the laser dwell time onto the laser process was theoretically studied by a simplified temperature field calculation. In finite difference method the time dependent heat conduction equation was considered exemplarily on tungsten material. For calculation, the temporal pulse profile of the laser beam was assumed as a Gaussian beam with a laser dwell time of 93 ns (Fig. 1), which was referred to a scan speed of 13,500 m/min. The irradiated cw laser power of 330 W onto the sample surface corresponds to a laser intensity of $9.5*10^7$ W/cm^2.
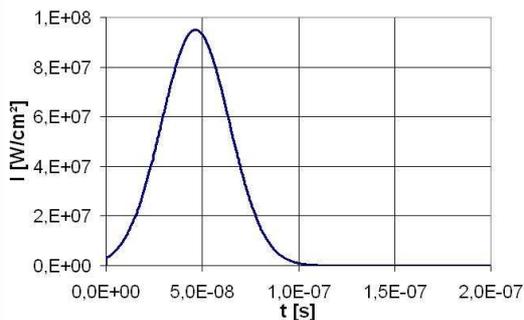

Fig. 1: Temporal pulse shape considered as Gaussian beam with a laser dwell time of 93 ns.

As shown in Fig. 2, temperature simulation elucidate the evaporation temperature of tungsten (5828 K) was not reached in spite of high impinged laser intensities.
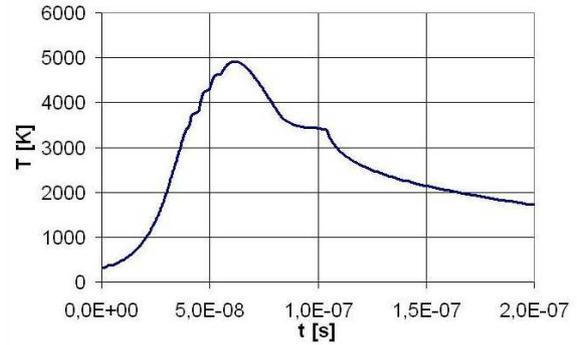

Fig. 2: Calculated temperature profile on tungsten within the laser focus centre.

Contrary to theoretical considerations, laser processing using the simulation parameters exhibits a partial material ablation, obviously in Fig. 3 as a line of dots.

Fig. 3: Digital photograph of laser processed tungsten surface, v = 13,500 m/min, P = 330 W, 1 scan.

Subsequently the temperature calculation was revised. Instead of the ideal tungsten surface with a reflectivity of R = 0.59, a technical surface with R = 0.2 was taken into calculation. Therefore a temperature rise exceeding the evaporation temperature of tungsten was obtained. According to the calculated temperature profile, ablation depths due to material evaporation and molten layer thicknesses were estimated of 50 nm and 800 nm, respectively. Thus, the simulation outcomes correlate to the experimental results obtained. Consequently, locally induced material evaporation due to high absorptivity centres and surface defects can be assumed.

Laser processing using 990 W laser power corresponds to a irradiated laser intensity of $2.85*10^8$ W/cm^2. A steady ablation groove achieved with a processing speed of 13,500 m/min illustrates Fig. 4. In that case the ablation width at the surface of 28 µm was broader as the laser spot size of 21 µm.
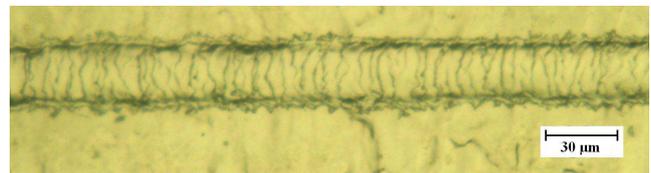

Fig. 4: Digital photograph of laser processed tungsten surface, v = 13,500 m/min, P = 990 W, 1 scan.

Temperature calculations conducted as described before result in 650 nm deep and 25 µm wide melting layers and 50 nm deep ablation gaps. A higher temperature gradient exists due to the higher impinged laser intensity.

Alternatively, laser irradiation of laser power of 330 W but otherwise a lowered processing speed of 4,500 m/min

yield uniform ablation cavities (Fig. 5). In this case laser dwell time was calculated onto 280 ns.
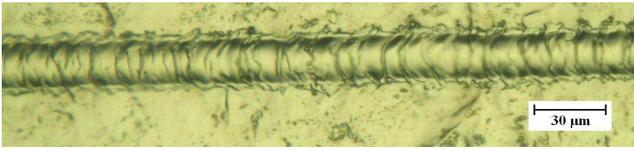

Fig. 5: Digital photograph of a laser processed tungsten surface, v = 4,500 m/min, P = 330 W, 1 scan.

According to the temperature calculation, a melting layer of 1 µm thickness was assumed. In contrast to results shown in Fig. 4, the width of the ablation cavity corresponds to the laser focus diameter of 21 µm due to the lowered irradiated intensity and correlates to the outcomes of theoretical temperature considerations.

Results demonstrated that a simplified temperature calculation by considering pulsed laser irradiation supplies a good agreement between theoretical values and experimental outcomes. In future enhanced temperature calculation will be carried out using a model with deflected laser beams.

3.2 Considerations of cw laser ablation using ultra fast scan speed

Depending on irradiated laser power, near-surface ablation widths became considerably wider than the laser focus spot size (Fig. 4, 6 left). The melting zone was broadened with increasing laser energy input due to either higher impinged laser power or reduced scan speed or both. In each case the energy input per unit section as the quotient of irradiated laser power and scan speed was increased. The broadening effect was also confirmed by the simulation outcomes. The width of the melting zone of the ablated cavity in Fig. 6 was measured of approx. 45 µm. Considering the applied processing parameters in theoretical calculations, the width of the melting zone was determined of 26 µm. Further the analyses of high speed camera photographs indicate the strong plasma formation at high scan speeds as a considerably influencing part.
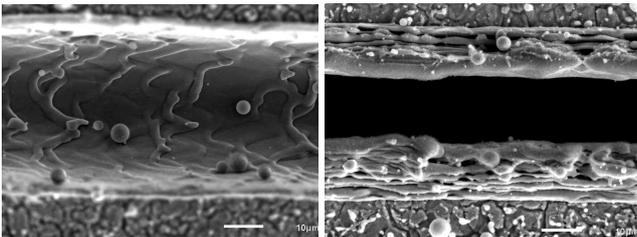

Fig. 6: SEM images of laser processed stainless steel surface, P = 660 W, v = 4,500 m/min, left 10 scans, right 25 scans.

Ablation products were observed in gaseous and liquid mixed phase regimes, whereas the ratio of the melting grows with increasing ablation depths. Due to the high surface tension, the ejected molten material re-solidified into small spheres with diameters ranging between 1 and 5 µm. The higher the scan speed the smaller the sphere diameter. The molten material was ejected out of the ablated cavity against the scan direction due to the formation of a backwards directed vapour-gas channel. With deeper ablation depths a higher amount of re-solidified material was deposited in layers onto the cavity sidewalls. As a result little cutting gaps much smaller than the laser focus spot size with widths between 16 µm (Fig. 6, right) and 3 µm (Fig. 17) as the smallest ones were obtained.

3.3 Ablation behaviour of stainless steel 1.4301

First investigations were carried out utilising the galvo scanner at a scan speed of 1,200 m/min (Fig. 7, 8). Figure 7 reveals a highly reliable ablation process up to ten scans and 200 µm ablation depths. Results obtained indicate a laser power threshold of a least 1.5 kW to achieve ablation depths considerably deeper than 500 µm at high processing speed. A further increase of the irradiated laser power from 1.76 kW to 2.65 kW did not enhance the ablation rate adequately. The effective cutting speed to cut a metal sheet of 0.5 mm thickness was determined of 60 m/min, applying 20 scans at a laser power between 1.32 kW and 2.64 kW. In contrast to reported results achieved at a scan speed of 900 m/min [1], with 1,200 m/min a 25% lowered effective cutting speed was obtained.
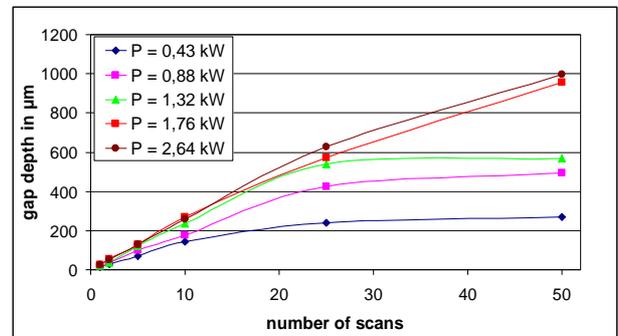

Fig. 7: Gap depth vs. scan number and laser power in 1 mm thick stainless steel, processing speed v = 1,200 m/min, galvo scanner.
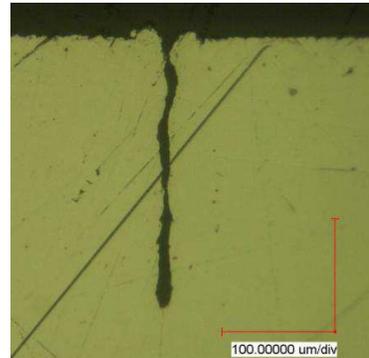

Fig. 8: Cutting gap in 1 mm thick stainless steel, P = 430 W, processing speed v = 1,200 m/min, 25 scans, galvo scanner.

Fig. 9 exhibits the required energy input per unit section to achieve a designated ablation depth depending on irradiated laser power; the energy per unit section was cumulated with the scan number. A significant decrease of the process efficiency at higher applied laser power is obviously. Accordingly, ablation depth of 100 µm can be achieved impinging a minor laser power of 430 W and 140 J/m accumulated energies per unit section respectively. However, application of 2.64 kW laser power requires an accumulated energy input per unit section of about 550 J/m. Furthermore a disproportional increase of the required accumulated energy input can be observed above a threshold

3

value, such as a laser power of 430 W at 150 µm ablation depth. As far as the threshold value the gap depth increases linearly with the impinged accumulated energy, and a homogeneous ablation process independent from the ablation depth can be assumed. Subsequently the ablation process became progressively less efficient and ablation depth increases insignificantly up to 250 µm in spite of high irradiated laser energy per unit section.
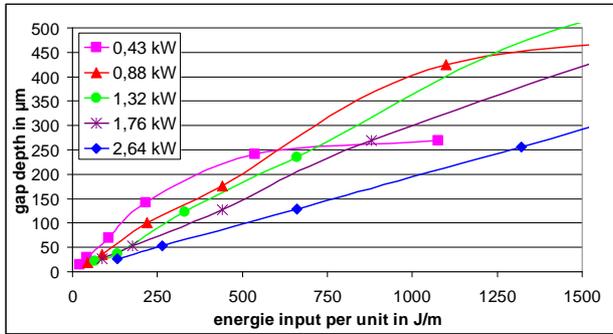

Fig. 9: Gap depth vs. energy input per unit section and laser power in 1 mm thick stainless steel, processing speed v = 1,200 m/min, galvo scanner.

The first experimental outcomes of investigations using an ultra fast polygon scanner unit summarises Fig. 10. Qualitatively the results conform to results obtained with the galvo scanner in spite of extremely short laser dwell times of 70 ns in minimum at a ultra fast scan speed of 18,000 m/min. The maximal achievable ablation depths were determined of 80 µm and 115 µm for 330 W and 500 W laser power, respectively and 100 scans at 13,500 m/min scan speed. At higher applied laser power the limit of achievable ablation depth was not specified due to insufficient scan numbers.
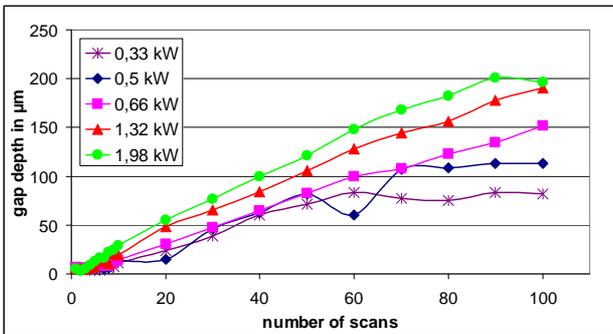

Fig. 10: Gap depth vs. scan number and laser power in 1 mm thick stainless steel, processing speed v = 13,500 m/min, polygon scanner.

The analysis of the accumulated energy input per unit section, shown in Fig. 11, implies good qualitatively and quantitatively agreements with results achieved using the galvo scanner at 1,200 m/min scan speed. In both cases and 1.32 kW irradiated laser power an energy input per unit section of 280 J/m was required to achieve ablation depths of about 100 µm.

As shown in Fig. 12, the ablation rate per scan number decreases with increasing scan speed. At a laser power of 1.32 kW a maximal ablation depth of 550 µm was achieved. The effective processing speed with due regards to scan numbers and 100 µm ablation depths was approx.

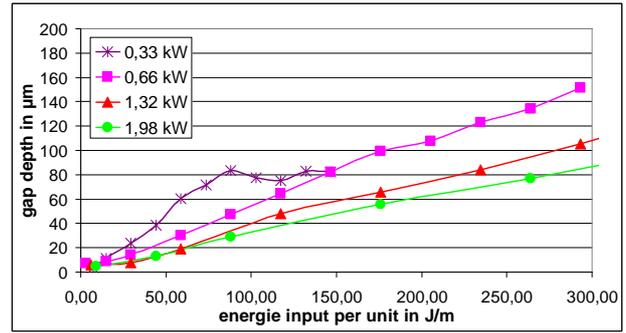300 m/min in maximum, investigated for processing speeds ranging between 1,200 and 18,000 m/min.

Fig. 11: Gap depth depending on energy input per unit section in 1 mm thick stainless steel, processing speed v = 13,500 m/min, polygon scanner.
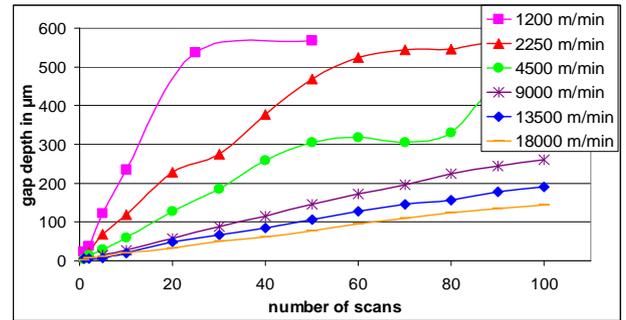

Fig. 12: Gap depth vs. scan number, 1 mm thick stainless steel, laser power P = 1.32 kW, polygon scanner.

The required energy per unit section to achieve ablation depths of 100 µm was determined constant of 280 J/m almost independent from scan speeds, obviously in Fig. 13. Only at deeper ablation depths a variance of the values was observed.
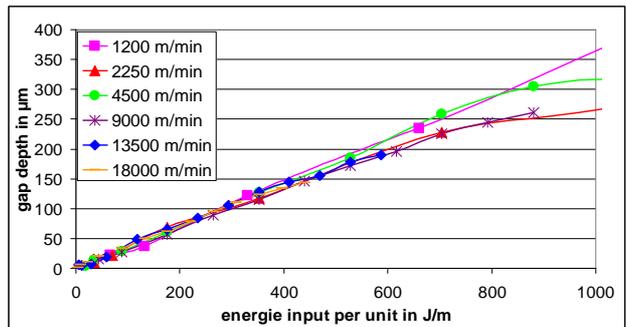

Fig. 13: Gap depth vs. energy input per unit section, 1 mm thick stainless steel, laser power P = 1.32 kW, polygon scanner.

The volume-ablation rate depended on ablation depth, impinged laser power and scan speed; it decreases with increasing ablation depth and scan speed, and increases with higher irradiated laser power. The volume-ablation rates fluctuates at 900 m/min scan speed between 900 and 2,400 mm³/min, at 2,250 m/min scan speed between 300 and 1,800 mm³/min, and at 18,000 m/min scan speed between 60 and 1,200 mm³/min. Thus, the ablation efficiency was increased up to an optimum value due to a higher amount of melting, which enhances the ablation process. Irradiation of higher laser power led to a stronger material evaporation accompanied by lowered ablation rates.

3.4 Laser ablation of copper and tungsten

Furthermore laser ablation of copper and tungsten was investigated, and referred to results achieved on stainless steel. Both materials are characterised by extreme material properties; a high reflectivity and high heat conductivity on copper and high melting and evaporation temperatures on tungsten. In contrast, stainless steel is characterised by less heat conductivity and a considerably lowered ablation threshold in comparison to copper and tungsten.

As shown in Fig. 11, on stainless steel ablation depths of 80 µm were obtained with a laser power of 0.33 kW and a scan speed of 13,500 m/min. The same laser processing parameter irradiated onto copper and tungsten surfaces cause inconsistent ablation behaviours. As recently as the double of the laser power up to 0.66 kW, ablation depths between 50 and 60 µm were obtained (Fig. 14, 15).
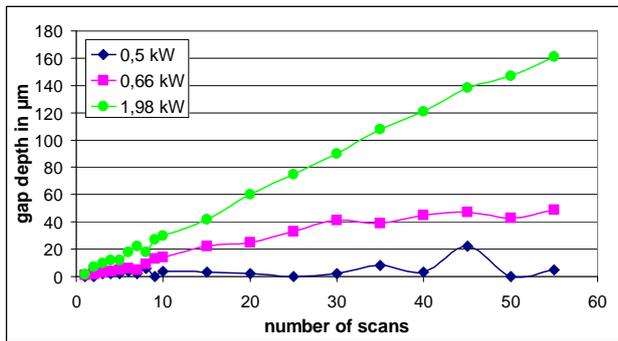

Fig. 14: Gap depth vs. scan number and laser power, 1 mm thick copper, processing speed v = 13,500 m/min, polygon scanner.
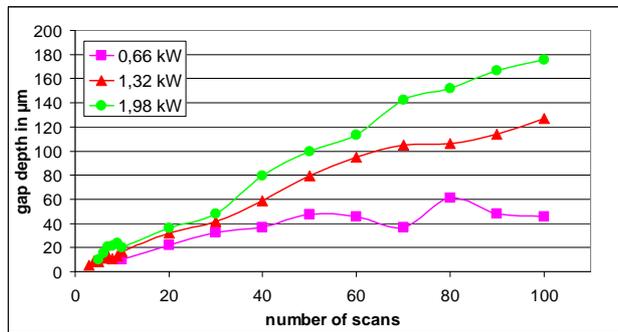

Fig. 15: Gap depth vs. scan number and laser power, 0.5 mm thick tungsten, processing speed v = 13,500 m/min, polygon scanner.

The achieved volume-ablation rate and ablation depth on stainless steel at laser processing parameters mentioned before and 50 scans was 5 and respectively 2 times higher compared to copper and tungsten (Table 4).

Table 4: Gap depth and ablation rate obtained on stainless steel, copper and tungsten; v = 13,500 m/min, P = 0.66 kW, 50 scans.

	Stainless steel	Copper	Tungsten
gap depth in µm	82	43	47
volume ablation rate in mm³/min	318	60	54

At higher irradiated laser power of 1.98 kW Table 5 illustrates equalised ablation rates per scan. Ablation depths per scan were observed between 2 and 3 µm, and even on copper the highest ablation depth was detected. At the higher laser power the volume-ablation rate on stainless steel was only increased by factor of 3 and 4 related to copper and tungsten respectively.

Table 5: Gap depth and ablation rate obtained on stainless steel, copper and tungsten, v = 13,500 m/min, P = 1.98 kW, 50 scans.

	Stainless steel	Copper	Tungsten
gap depth in µm	121	149	99,7
volume ablation rate in mm³/min	990	318	234

The seeming contrast between the considerably higher volume-ablation rate on stainless steel compared to copper and tungsten at otherwise approximately similar ablation depths is explainable considering the widths of the ablated cavities. At high irradiated laser power, on stainless steel significant broader ablation widths were observed. Therefore a significantly lowered deposition of molten material onto the sidewalls of the ablated cavities in stainless steel can be assumed compared to copper and tungsten.

3.5 Laser micro structuring

Fig. 17 and 18 illustrate laser generated micro structures obtained on stainless steel using the polygon scanner and ultra fast scan speed at different scan numbers. In Fig. 17 the distance between the single cavities was 25 µm. The width of 13 µm near the surface was considerably smaller than the focus spot size. Re-deposition of molten material onto the walls of the ablation cavities lifts the height of the walls over the height of the not irradiated surface.
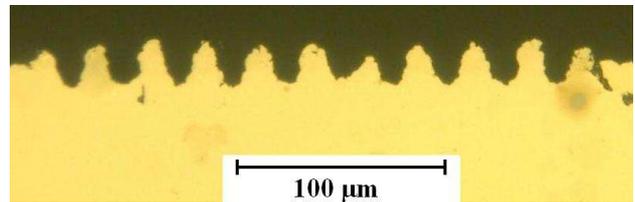

Fig. 17: Digital image of periodically ablated cavity structure, stainless steel, v = 12,000 m/min, P = 330 W, 15 scans.

Previously, applying a scan speed of 900 m/min separate micro walls of 37 µm lateral distances were achieved [1, 2]. With increasing scan speed, smaller lateral distances between the single lines were obtained accompanied by a significant higher resolution of the micro structures.

Fig. 18 illustrates an alternating wall – gap micro structure with a depth of 50 µm, obtained after 60 scans. The widths of the gaps decrease up to 3 µm due to re-deposition of molten material.
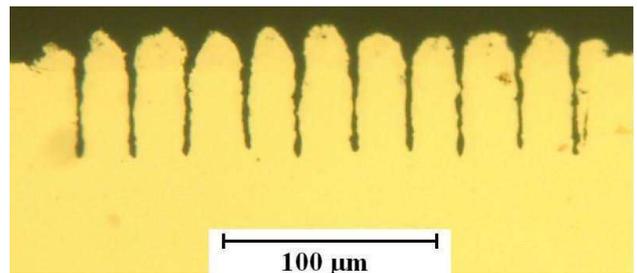

Fig. 18: Digital image of periodically ablated cavity structure, stainless steel, v = 12,000 m/min, P = 330 W, 60 scans.

However, the mechanism of the laser energy input into the extremely small gaps under irradiation of a laser beam with a laser spot size of 21 µm is still under discussion.

3.6 Applications

- Laser micro structuring of metal surfaces

Fig. 19 illustrates a detailed micro wall array generated in stainless steel with a width of 35 µm, a lateral distance of 37 µm and aspect ratio of 1:3. The area processing rate was 168 cm²/min; increased rates can be obtained at less scan numbers and lowered ablation depths.
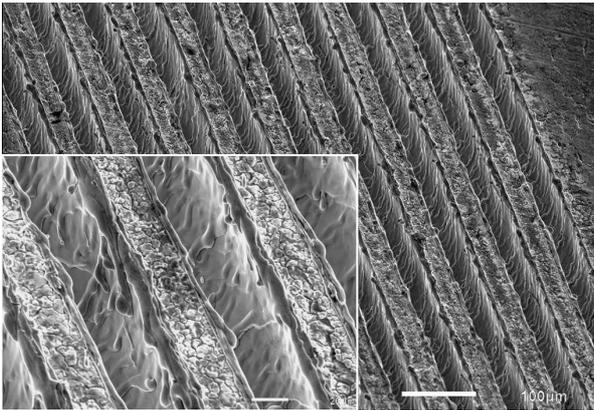

Fig. 19: SEM image of micro structured stainless steel surface, v = 1,200 m/min, P = 880 W, 5 scans.

- Thin film ablation

Another approach studied ultra fast laser ablation of 2 µm thick CrNi layer, deposited onto a glass substrate (Fig. 20). Residue-free laser ablation was achieved applying 2 laser scans with 0.88 kW laser power and a scan speed of 9,000 m/min. The area processing rate was determined of 2,250 cm²/min. Advantageous potential of the novel technology indicates the enormous area processing rate of 4,500 cm²/min, calculated for a grid fabrication with a period of 100 µm.
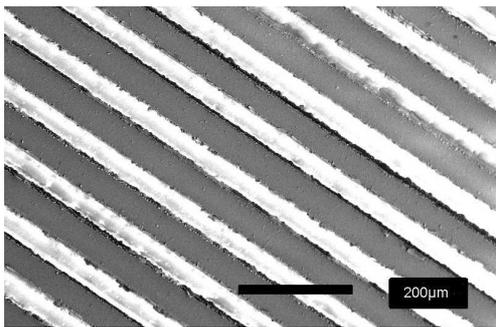

Fig. 20 SEM image, thin film ablation of NiCr layer, thickness: 2 µm, P = 880 W, v = 9,000 m/min, 2 scans.

- High rate laser cutting

Application of the high rate ablation laser technology in laser ablation cutting enables high detailed outlines due to the short laser dwell times. Fig. 21 (left) illustrates an acute-angled outline with an edge radius of 30 µm in stainless steel. On right side a machining example with a cutting length of 560 mm and 0.3 mm thickness is shown. The total processing time was 3 sec. according to an effec-

tive processing speed of 112 m/min. In contrast laser cutting of the structure using conventional laser cutting technologies and flying cutting optics takes at least ten times longer.
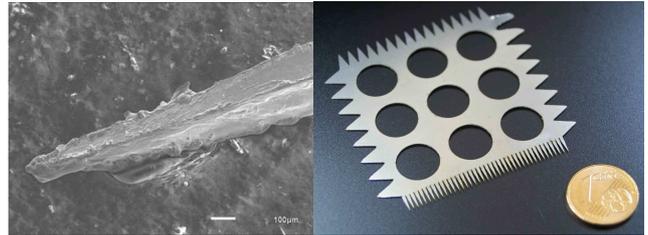

Fig. 21: left: SEM image of 5° tip in stainless steel, P = 1,76 kW v = 600 m/min, 2 scans**; right:** processing example in stainless steel, thickness 0.3 mm, scan length: 560 m , 10 scans.

4. Summary and outlook

In the study, for the first time laser micro structuring applying ultra fast scan speeds up to 18,000 m/min joint together with high brilliant high power cw fibre laser was presented. Especially for thin metal sheet processing with thicknesses smaller than 100 µm a high potential of the ultra fast technology can be assumed. Laser cutting of stainless steel and copper metal sheets of 50 µm thickness were carried out with 700 m/min effective cutting speed at 2 kW laser power; for tungsten the effective cutting speed was 540 m/min. Furthermore application examples in laser micro structuring of surfaces, thin film ablation and high rate laser ablation were presented.

Prospective works will be themed onto ultra fast beam switching of the high power cw laser radiation as soon as a more detailed scientific investigation of the interacting effects using high power cw lasers in high rate laser micro processing.

References
[1] R.Ebert, L.Hartwig, F.Peuckert, S.Kloetzer, J.Schille, T. Hagemann, S.Wischmann, H.Exner: "High rate ablation with 3 kW single mode fibre laser", Proceedings of the 5. Int. WLT-Conference on Laser in Manufacturing, June 2009, Munich, Germany, pp.565-570.
[2] L.Hartwig, R.Ebert, S.Kloetzer, S.Weinhold, J.Drechsel, F.Peuckert, J.Schille, H.Exner: "Material processing with a 3kW single mode fibre laser", Proceedings of LAMP2009 - the 5th International Congress on Laser Advanced Materials Processing, June 29 – July 2, Kobe, Japan, TuPH-3(#153).
[3] L.Hartwig, R.Ebert, F.Peuckert, S.Kloetzer, A.Streek, J.Schille, U.Loeschner, H.Exner: "Hochleistungs-Lasermikrobearbeitung mit brillanter cw-Laserstrahlung" (written in German), 20th International Scientific Conference Mittweida, Oktober 28-29, Scientific Reports Nr. 4, 2009, S. 57-64.